Journal of Dermatological Science 94 (2019) 276–283

Contents lists available at ScienceDirect

Journal of Dermatological Science

journal homepage: www.jdsjournal.com

Original Article

Transcriptomic analysis of human dermal fibroblast cells reveals potential mechanisms underlying the protective effects of visible red light against damage from ultraviolet B light

Hyun Soo Kim[a], Yeo Jin Kim[a], Su Ji Kim[a], Doo Seok Kang[a], Tae Ryong Lee[b], Dong Wook Shin[c,*], Hyoung-June Kim[b,*], Young Rok Seo[a,*]

[a] Department of Life Science, Institute of Environmental Medicine, Dongguk University Biomedi Campus, 32, Dongguk-ro, Ilsandong-gu, Goyang-si, Gyeonggi-do, 10326, Republic of Korea
[b] Bioscience Research Institute, Amorepacific Corporation R&D Center, 1920, Yonggu-daero, Giheung-gu, Yongin-si, Gyeonggi-do, 17074, Republic of Korea
[c] College of Biomedical & Health Science, Konkuk University, Chungju, 27478, Korea

ARTICLE INFO

Article history:
Received 23 July 2018
Received in revised form 19 March 2019
Accepted 20 March 2019

Keywords:
Visible red light
Protective effect
RNA-seq
Ranscriptomic analysis

ABSTRACT

Background: Ultraviolet B (UVB) radiation is a major cause of skin photodamage, including the damage associated with photodermatoses, aging, and cancer. Although many studies have shown that red light has photoprotective effects on skin, the mechanisms underlying these effects are still poorly understood.
Objective: The aim of this study was to identify the photoprotective effects of visible red light against UVB-induced skin damage in normal human dermal fibroblast cells using a transcriptomic approach.
Methods: Next-generation sequencing-based transcriptomic analyses were used to profile transcriptomic alterations and identify genes that are differentially expressed by visible red light and by UVB exposure. To understand the biological networks among identified genes, a literature-based biological pathway analysis was performed. Quantitative real-time polymerase chain reaction assays were used for mRNA-level validation of selected key genes.
Results: We observed that visible red light contributes to skin cell protection against UVB by modulating gene expression that enhances the adaptive response to redox and inflammatory balancing and by upregulating genes involved in DNA excision repair processes. We also identified that several key genes in the red light-induced biological network were differentially regulated.
Conclusions: Visible red light enhanced the UVB-protective effects in normal human skin cells *via* the transcriptomic modulation of genes involved in cell-protective processes. Our findings from this next-generation sequencing analysis may lead to a better understanding of the cytoprotective effects of visible red light and provide direction for further molecular or mechanistic studies.

1. Introduction

The harmful effects of routine exposure to extrinsic stressors have always been an issue in global public health. One major stressor, ultraviolet (UV) radiation, has deleterious effects on the skin, including sunburn, erythema, photodermatoses, aging, and cancer [1]. Physically, UV irradiation of DNA causes highly mutagenic photoproducts, such as cyclobutane-pyrimidine dimers and (6-4) photoproducts [2]. Numerous studies have demonstrated that as the number of these UV-induced DNA lesions increases, there is an increased likelihood of mutations in key genes that can result in cell death or can even accelerate carcinogenesis if the mutation occur in cancer-regulating genes [3–5]. Additionally, ultraviolet B (UVB) radiation induces reactive oxygen species production, which causes direct and indirect free radical damage to nucleotides, such as the formation of 8-hydroxy-2′-deoxyguanosine [6,7]. Diverse studies have investigated the crucial protective roles of several repair pathways against UV-induced DNA damage, emphasizing that the enhancement of these repair processes is vital for combating skin damage by UV irradiation [8–10].

Various studies have reported the protective effects of red light against stress-induced damage. Low-intensity red laser treatment reportedly counteracts damage by extrinsic stressors, including UV radiation and harmful chemicals, by inducing adaptive responses [11,12]; it also facilitates wound healing by fibroblasts by stimulating cell proliferation and growth [13,14]. In addition, *in*

* Corresponding author.
E-mail address: biocosmed@kku.ac.kr (D.W. Shin).

https://doi.org/10.1016/j.jdermsci.2019.03.003
0923-1811/

vivo photorejuvenation studies have demonstrated that red light irradiation enhances the healing of skin injuries [15,16]. Besides these beneficial effects, gene expression profiling of low-intensity red laser-irradiated human skin cells has been studied to identify possible underlying mechanistic changes [17]. However, little is currently known about the cellular benefits of visible-wavelength red light, particularly in terms of transcriptomic data.

Transcriptomic expression profiles reflect the physiological condition and functional stages within an organism. Various transcriptomic approaches have been taken to identify intracellular mechanistic changes under certain conditions. Recently, with the remarkable improvement of high-throughput next-generation sequencing (NGS) techniques, RNA-sequencing (RNA-seq) now allows for the analysis of allelic variations as well as gene expression profiles with unprecedented scale and speed [18,19]. The development of various bioinformatic tools has facilitated the generation of significant scientific findings and the archival of large amounts of data from RNA-seq studies. Text mining-based biological signaling network analysis is a bioinformatics approach that can yield meaningful interpretations of mRNA expression profiles.

Herein, we conducted NGS-based transcriptional profiling of visible red light- and UVB-treated normal human dermal fibroblasts (NHDFs) to better understand the biological pathways underlying the protective effects of red light against UVB exposure. Biological signaling pathways based on the identified transcriptomic profiles were analyzed using text mining technique-based software. Our data may provide insights into the potential mechanisms of the protective effects of visible red-light irradiation against UVB irradiation-induced skin injuries.

2. Materials and methods

2.1. Cell culture and light treatment

NHDFs were purchased from Lonza (Basel, Switzerland). NHDFs were cultured in Dulbecco's modified Eagle medium (DMEM), with 4.5 g/L glucose, L-glutamine, 10% fetal bovine serum, and 1% penicillin-streptomycin mixture (Gibco, USA), at 37 in a 5% CO_2 incubator. Light irradiation was conducted with UVB (312 nm) at 0.1 J/cm^2 and visible red light (620–690 nm; λ_{max} =660 nm) at 60 J/cm^2 according to the procedure in our previous study [20]. During the light treatment, continuous-wave irradiation was performed. The state of energy density/irradiance of visible red light was 16.67 mW/cm^2, and the exposure time was 60 min. The cells were irradiated in the media without phenol-red and with the indicated doses of each light. There were six groups based on the light treatment type and post-incubation duration: (1) 'Control' group; (2) the 'Red' group; (3) 'UV-1h' group; (4) 'Pre-Red-1h' group; (5) "UV-4h" group; and (6) "Pre-Red-4h" group. The detailed experimental design for the light treatment is explained in Supplementary Fig. 1.

2.2. mRNA sequencing and identification of differentially expressed genes (DEGs)

NHDF cells were harvested, and mRNA was extracted using RNeasy mini kits (Qiagen, USA) in accordance with manufacturer's instructions. The quality of the extracted mRNA was evaluated using an Agilent Bioanalyzer Nano Chip 2100 (Agilent Technologies, USA). The RNA-seq experiments and data analysis were conducted by Macrogen (Korea). Purified mRNA was fragmented, and pair-end RNA sequencing was conducted using a HiSeq2000 (Illumina, USA) sequencing system for the 1-h pretreatment set and a HiSeq2500 (Illumina) system for the 4-h pretreatment set. TruSeq Stranded mRNA LT Sample Prep kits (Illumina) were used to establish libraries according to the sample preparation guide. To estimate RNA expression profiles, the RNA-seq reads were mapped with a human reference genome (hg19) using TopHat [21]. Human reference genome sequence and annotation data were downloaded from the University of California, Santa Cruz (UCSC) Genome Browser (http://genome.uscs.edu). The assembly of mapped reads was performed by Cufflinks [22], and default options and transcript abundances were estimated in fragments per kilobase of exon per million fragments mapped (FPKM). Data with |fold-change| $\geq$ 1.5 and p-value < 0.05 were considered differentially expressed. All of the datasets are available at the Gene Expression Omnibus (GEO) repository: GSE116968

2.3. Biological pathway analysis

We used Pathway Studio version 12.0 (Elsevier, USA) to analyze the biological pathways involved in our differential gene expression dataset. Pathway Studio, with its database derived from a text-mining technique [23], helped to analyze the interactions between each DEG, identify related cellular processes and diseases, and also helped in the production of schematic pathways among them. All of the networks among entities such as proteins, functional classes, cell processes and diseases were carefully curated based on their connectivity among other entities and number of references that prove their relationships.

2.4. Quantitative real-time polymerase chain reaction (qRT-PCR)

qRT-PCR was performed validate transcript levels. Total RNA was extracted from NHDFs using the RNeasy Mini kit (Qiagen), according to the manufacturer's instructions. For cDNA synthesis with the ImProm-II^{TM} Reverse Transcription System (Promega, USA), 500 ng of RNA was used, in accordance with the manufacturer's instructions. Gene-specific primer sequences were designed by Integrated DNA Technologies (USA) and are listed in Supplementary Table 1. qRT-PCR was performed using SYBR Premix Ex Taq (Takara, Japan) with 100 nmol of each primer in a Rotor-Gene Q Real-Time PCR system (Qiagen). Thermal cycling conditions comprised initial denaturation at 95 for 5 min, followed by 45 cycles at 95 for 10 s, 60 for 12 s, and 72 for 60 s. The data were analyzed using Rotor-Gene Analysis Software (Corbett Research, Australia); all transcript levels were normalized to glyceraldehyde 3-phosphate dehydrogenase as an internal control gene according to the $2^{-\Delta\Delta C}{}_T$ method [24]. The mRNA expression levels were indicated as fold-changes relative to the control levels.

2.5. Statistical analysis

All graphical data are presented as means ± standard deviation. All data were obtained from at least three independent experiments conducted in triplicate. Between groups comparison were analyzed using the Student's t-test; and comparisons among more than two groups were analyzed using ANOVA. P-values < 0.05 were considered statistically significant.

3. Results

3.1. Identification of DEGs in NHDFs

We obtained transcriptome profiles of NHDFs that had been exposed to visible red light and UVB. We classified them into the following six groups: Control, Red, UV-1h, Pre-Red-1h, UV-4h, and Pre-Red-4h. The upregulation/downregulation patterns of genes were as follows: Red group: 176 genes upregulated, 57 genes downregulated; UV-1h group: 30 upregulated, 33 downregulated;

UV-4h group: 180 upregulated, 342 downregulated; Pre-Red-1h group: 176 upregulated, 110 downregulated; and Pre-Red-4h group: 358 upregulated, 474 downregulated. Supplementary Fig. 2 shows each DEG profile as a volcano plot.

3.2. Identification of cellular effects induced by visible red light through signaling pathway analysis based on transcriptomic alterations in NHDFs

To determine the biological effects of visible red light exposure on NHDFs, we established a visible red light-induced biological pathway (Fig. 1A). To ensure confidence in our results, we excluded relations between entities (proteins, small molecules, cell processes, and diseases in the figure) that have number of references below three during the analysis. Moreover, we focused on the associated cell processes and functional classes among DEGs to explore their biological influences. Particularly, a 'functional class' in Pathway Studio provides information about the classified function of genes based on Gene Ontology data. According to the established pathway shown in Fig. 1A, DEGs mainly contributed to the enhancement of cell processes, including cell damage and DNA damage responses, and the modulation of the inflammatory, oxidative stress, and wound healing responses. In addition, functional classes among the upregulated genes were involved in oxidative stress restoration, cell growth regulation, and inflammatory responses. To uncover more detailed networks among the key factors, we selected meaningful genes based on the value of connectivity ratio (>0.7). The connectivity ratio is an importance score for each entity based on comparing literature-based data and analyses with local connectivity data in established pathways. We selected the following genes that appear to be involved in the biological effects of visible red light on skin cells based on our pathway analysis: heat shock protein family A (Hsp70) member 1A (HSPA1A), Hsp70 member 5 (HSPA5), prostaglandin-endoperoxide synthase 2 (PTGS2), interleukin-6 (IL-6), leukemia inhibitory factor (LIF), heme oxygenase (HMOX), activating transcription factor 3 (ATF3), growth arrest and DNA damage-inducible alpha (GADD45A), and growth arrest and DNA damage-inducible beta (GADD45B).

Upregulation of the HSPA gene family (HSPA1A, and HSPA5) was observed, and HSPA1A had the highest connectivity in an analyzed pathway (Fig. 1A). Considering the stress-responsive cytoprotective function of heat shock proteins [25], visible red light may induce the activation of cytoprotective signals against cell stressors. In the analyzed pathway, HSPA1A was also involved in attenuating skin photodamage and photoaging under red light exposure. PTGS2 and HMOX, which belong to the oxygenase pathway and are involved in redox balancing [26,27], were also upregulated. This result suggests that visible red light may enhances oxidative stress-response signaling. DEGs were significantly correlated with several DNA repair processes, particularly DNA excision repair-related pathways, with numerous interactions with the upregulated genes GADD45A, GADD45B, and ATF3.

3.3. Identification of cellular effects of visible red light pretreatment in UVB-exposed NHDFs through signaling pathway analysis

To understand the cellular effects of red light pretreatment against UVB exposure, we established the significance pathway among identified DEGs from the Pre-Red group compared to the UV group (Fig. 1B). The pathway analysis suggested that transcriptomic changes induced by pretreatment of visible red light may enhance cellular processes involved in oxidative stress responses, wound healing, inflammation, and DNA damage responses. To compare the cellular effects of gene expression modulation in each group, we summarized the cellular processes, functional classes, and related gene lists obtained from pathway analysis (Table 1). DNA excision repair-related cell processes, including gap-filling, nucleotide excision repair, DNA modification, DNA repair, and DNA damage excision were combined into the "Response to DNA damage". We observed that the cellular pathways and functional classes were generally similar with several common DEGs in the red light-only group (Red/Control) and the red light pretreatment group (Pre-Red-4h/UV-4h).

We also found that visible red light enhanced oxidative stress responses, wound healing, and DNA repair-related cellular processes against UVB-induced damage at 1-h post-incubation after UVB treatment (Supplementary Fig. 3A). Details of the pathway and the related DEG lists were different for each group; however, the overall cell processes involved were similar in two of the post-incubation groups (Supplementary Fig. 3B). Pretreatment with visible red light predominantly enhanced cell protection against UVB-induced impacts.

3.4. Prediction of potential underlying mechanisms of the photoprotective effects of visible red light against UV exposure

To explore the potential mechanisms underlying the protective effects of visible red light pretreatment under UV exposure, we compared the pathway of visible red light-only irradiation (Fig. 1A) and that of visible red light treatment before UVB exposure (Fig. 1B). The combined pathway comprised entities that were present in both pathways, such as genes, cell processes, diseases, functional associations, and various interactions. We explored 18 upregulated genes associated with the effectiveness of visible red light protection against UVB exposure and changes in inflammatory cytokines and cell damage responses, such as mitogen-activated protein kinase, which is important for the inhibition of UVB-induced skin photodamage and photoaging (Fig. 2A). Further, we also observed that commonly altered genes, such as ATF3, IL-6, and HSPA1A induce the enhancement of ATF2-GADD45A-PCNA-APEX1-mediated DNA excision repair pathways (Fig. 2A, green highlights). These findings suggest that visible red light protects skin against UVB-induced damage by enhancing DNA repair processes and increasing cell damage-attenuating responses.

Based on our findings, we simplified the pathway by careful curation of the connectivity among various entities and literature references of all paths using Pathway Studio (Fig. 2B). Key signaling networks among the six genes (HSPA1A, HSPA5, PTGS2, IL-6, LIF, and ATF3) were involved in the negative regulation of oxidative stress and inflammatory responses and the enhancement of DNA excision repair and wound healing. This pathway suggested a possible protective mechanism of visible red light in skin cells against UVB-induced cellular damage. We validated mRNA expression levels of the six key genes using qRT-PCR, and their upregulation/downregulation trends were similar to expression level changes in our RNA-seq analysis (Fig. 3).

4. Discussion

The beneficial effects of red light in attenuating UV-induced damage have been investigated and there is increasing scientific evidence supporting the use of red light in medical applications [28,29]. Therapeutic effects of diverse wavelength and light fluence of low-level red laser treatment on the skin have been reported [11,12,15,17]. However, the biological mechanisms underlying the beneficial effects of red light and the transcriptional responses to light in the visible spectrum remain unclear. To study the transcriptomic aspects of the protective effects of exposure to visible red light, we applied the same wavelength (660 nm) and

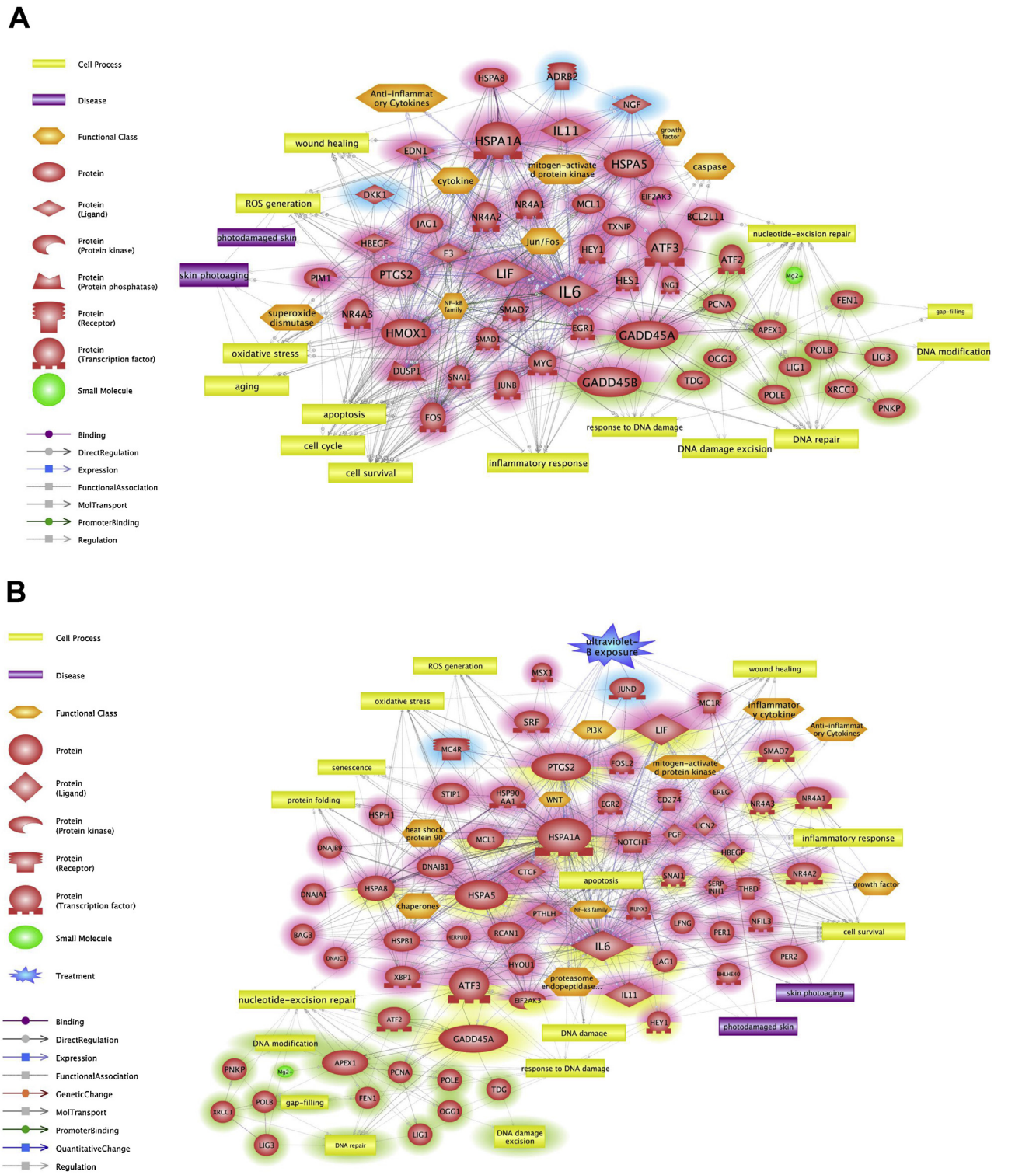

Fig. 1. Pathway analysis data revealing the biological signaling networks that underlie the response of NHDFs to visible red **light exposure. (A)** Biological pathways involving significant DEGs by visible red light irradiation. Selected key genes with connectivity are highlighted by increased entity size. **(B)** DEGs by pretreatment with visible red light and 4 h of post-incubation after UVB exposure. '+' or '–' at the end of the arrows in the pathway indicate positive/negative effects of each relations, respectively. Yellow highlights indicate DEGs in common for the red light-treated groups. Red and blue highlights indicate upregulated and downregulated genes, respectively. Green highlights indicate genes involved in DNA excision repair pathways. A schematic legend of the entities and relations (marked as arrows) in the pathway are provided on the left side of the figure. Circles and squares on the arrows in the schematic legend are included to improve visibility.

fluence (60 J/cm2) that showed significant photoprotective effects in NHDFs in our previous study [20].

As summarized in Table 1, we observed that wound healing, responses to DNA damage, and regulation of inflammatory and oxidative stress responses were enhanced by visible red light irradiation. Differential expressions of HSPA1A, HSPA5, PTGS2, IL-6, LIF, ATF3, GADD45A, and GADD45B were instrumental in identifying pathways given their common biological functions (Fig. 1A). The heat shock protein family genes HSPA1A and HSPA5 have protective functions against ultraviolet-induced skin damage,

Table 1
Summarized the cellular processes, functional classes, and related gene lists from pathway analysis data.

	Entity name	Related gene lists from pathways involved in each group		
		Red/Control DEGs pathway	Pre-Red-4h/UV-4h DEGs pathway	Common genes in the both pathways
Cell process	Aging	IL-6, HSPA1A, HMOX1	HSPB1, IL-6, NOTCH1, PTGS2, HSPA1A	HSPA1A, IL-6
	Apoptosis	EGR1, HSPA8, MYC, NR4A3, ATF3, MCL1, GADD45A, SNAI1, TXNIP, HSPA5, ADRB2, DKK1, NR4A1, DUSP1, HBEGF, EIF2AK3, FOS, GADD45B, PIM1, JUNB, NR4A2, SMAD7, SMAD1, JAG1, F3, HEY1, ES1	HSPA8, NR4A3, ATF3, CD274, MCL1, NFIL3, HSPA1A, STIP1, HSP90AA1, PTGS2, SNAI1, PTHLH, IL-6, DNAJC3, MSX1, DNAJB1, HSPA5, JUND, XBP1, RUNX3, NR4A1, HYOU1, EGR2, SRF, HBEGF, IL11, UCN2, EIF2AK3, THBD, CTGF, PGF, NOTCH1, HSPH1, NR4A2, SMAD7, JAG1, LIF, HERPUD1, HEY1, BHLHE40, RCAN1, BAG3, HSPB1, PER2, PER1	ATF3, EIF2AK3, HBEGF, HEY1, HSPA5, JAG1, MCL1, NR4A1, NR4A2, NR4A3, SMAD7, SNAI1
	Cell cycle	GADD45A, HSPA1A, DUSP1, JUNB, HMOX1, ATF3, IL-6, EGR1, SNAI1, NR4A1, MCL1, HES1, MYC, PIM1, GADD45B, HSPA8, FOS		
	Cell survival	HMOX1, HSPA1A, NR4A1, IL-6, JAG1, MYC, HSPA8, TXNIP, F3, ATF3, NR4A3, HSPA5, EIF2AK3, FOS, HBEGF, EGR1, PIM1, GADD45A, GADD45B, DUSP1, MCL1, SNAI1, DKK1, NR4A2	HSPA1A, NR4A1, IL-6, SRF, XBP1, PTHLH, JAG1, IL11, CTGF, HSPA8, NOTCH1, ATF3, NR4A3, HSPA5, EIF2AK3, HSPB1, HBEGF, LIF, PTGS2, PGF, CD274, BAG3, MCL1, SNAI1, NR4A2	ATF3, EIF2AK3, HBEGF, HSPA5, HSPA8, IL-6, JAG1, MCL1, NR4A1, NR4A2, NR4A3, SNAI1
	Response to DNA damage	TDG, ING1, HSPA1A, GADD45A, MYC, GADD45B, IL-6, ATF2, MCL1, ATF3	PTGS2, MC1R, IL-6, HSPA1A, MCL1, GADD45A, HSPA8, BHLHE40, PER2, ATF3	ATF3, GADD45A, HSPA1A, IL-6, MCL1
	Inflammatory response	F3, HMOX1, SMAD7, DUSP1, ADRB2, EGR1, NR4A1, ATF3, IL-6, HSPA1A, NR4A2	PTGS2, IL11, SMAD7, PGF, CTGF, CD274, NR4A1, XBP1, ATF3, IL-6, THBD, HSPA1A, NOTCH1, NR4A2, LIF, HSPB1	ATF3, HSPA1A, IL-6, NR4A1, NR4A2, SMAD7
	Oxidative Stress	EDN1, PTGS2, NGF, GADD45A, MYC, HSPA1A, IL-6, HSPA5, HMOX1	ATF3, HSPA1A, HSPA8, IL-6, HSPA5, EIF2AK3, JUND, PTGS2, NOTCH1, RCAN1, HSPB1, XBP1	HSPA1A, HSPA5, IL-6, PTGS2
	ROS generation	HSPA1A, MYC, EDN1, HSPA5, PTGS2, HMOX1, GADD45A, NGF, IL-6	HSPA1A, MCL1, HSPA5, EIF2AK3, PTGS2, HSPB1, HBEGF, IL-6	HSPA1A, HSPA5, IL-6, PTGS2
	Wound healing	HMOX1, HSPA1A, ADRB2, IL-6, EGR1, HBEGF, F3, SMAD7	HSPA1A, PTGS2, HSPB1, IL-6, HBEGF, HSP90AA1, CTGF, SMAD7, PGF, NOTCH1	HBEGF, HSPA1A, IL-6, SMAD7
Functional class	Anti-inflammatory Cytokines	HMOX1, IL-6, PTGS2	PTGS2, IL-6, IL11	IL-6
	Caspase	HMOX1, MCL1, MYC, ATF3, HSPA5, BCL2L11, PTGS2, HSPA1A,		
	Cytokine	FOS, F3, MYC, HMOX1, LIF, NGF, MCL1, IL-6, HBEGF, PTGS2, EGR1, PIM1, SMAD7, EDN1, ATF3, JUNB, HSPA1A, ADRB2, DUSP1		
	Growth factor	IL-6, EDN1, HMOX1, DUSP1, PIM1, LIF, PTGS2, EGR1, MCL1, F3, MYC, FOS, NR4A1	IL-6, PGF, CTGF, PTHLH, LIF, PTGS2, MCL1, NR4A1	LIF, MCL1, NR4A1, PTGS2, IL-6
	Jun/Fos	FOS, DUSP1, EDN1, IL-6, NR4A1, HMOX1, MYC, PTGS2, F3, EGR1, JUNB		
	Mitogen-activated protein kinase	IL-6, PTGS2, HBEGF, ADRB2, IL11, LIF, EGR1, EDN1, HSPA1A, ATF3, NR4A2, MYC, DUSP1, F3, NR4A1, FOS, SNAI1, MCL1, JUNB, HMOX1	NR4A2, IL-6, PTGS2, PER1, NOTCH1, CD274, CTGF, NR4A1, SNAI1, MCL1, ATF3, HSPA1A, PTHLH, HBEGF, MC4R, LIF	ATF3, HBEGF, HSPA1A, LIF, MCL1, NR4A1, PTGS2, SNAI1
	NF-kB	SMAD7, LIF, FOS, EGR1, SNAI1, F3, PTGS2, HMOX1, GADD45B, HSPA1A, MYC, IL-6, MCL1, EDN1, HBEGF, ADRB2, IL11, ATF3,	NR4A2, HSPA1A, NOTCH1, ATF3, HSPB1, SMAD7, RCAN1, THBD, HBEGF, CTGF, IL-6, HSPA5, PTGS2, EIF2AK3, BAG3, SRF, LIF, SNAI1, IL11, PGF, MCL1, CD274	ATF3, HBEGF, HSPA1A, IL11, IL-6, LIF, MCL1, PTGS2, SNAI1
	Superoxide dismutase	IL-6, HSPA1A, PTGS2, HMOX1		

including wrinkle formation [25,30]. Moreover, PTGS2, also known as cyclooxygenase 2 (COX-2), is crucial in the modulating redox, inflammatory, and anti-inflammatory responses [26]. These findings are also partly linked with inflammatory activation related to IL-6, LIF, and ATF3 activation. ATF3 exerts a modulatory effect on immune responses and is central to the cellular adaptive-response network [31]. Upregulation of the pro-inflammatory cytokine LIF also contributes to increased cell survival [32]. Indeed, appropriate levels of inflammatory responses during the early stages of immune responses are essential for protection from extrinsic stressors [33–35]. Based on this knowledge, we demonstrated that visible red light-induced transcriptomic changes promote the activation of cytoprotective processes and immune responses, and consequently induce adaptive responses against cellular damage. These findings also support our previous work, which identified the protective effects of and adaptive responses induced by visible red light against UVB-induced damage to skin fibroblast cells [20].

Although there is *in vitro* evidence regarding the UV-protective effect of red laser light, The full extent of the effects of visible-wavelength red light remain relatively unknown [11,12]. In the present study, we used transcriptomic analyses to elucidate the photoprotective effects of visible red light in human skin cells. Our result showed similarity of the involved cellular processes in the pathways as shown in Fig. 1B and Supplementary Fig. 3A, although the scale of the transcriptomic alterations differed between UV-1h and UV-4h exposures (Supplementary Fig. 2). The high-energy protons generated by UVB irradiation cause direct physical damage to DNA and proteins, thereby impairing several cellular functions [2]. Accordingly, we deduced late responses as large-scale transcriptomic changes by UVB exposure are the result of the early response to direct physical damage to DNA or proteins. Moreover, as summarized in Supplementary Fig. 3B, our findings also revealed that the cellular scale response induced by visible red light pretreatment may be similar to the early response induced by UVB energy. 4-h of post-incubation time after UVB irradiation was

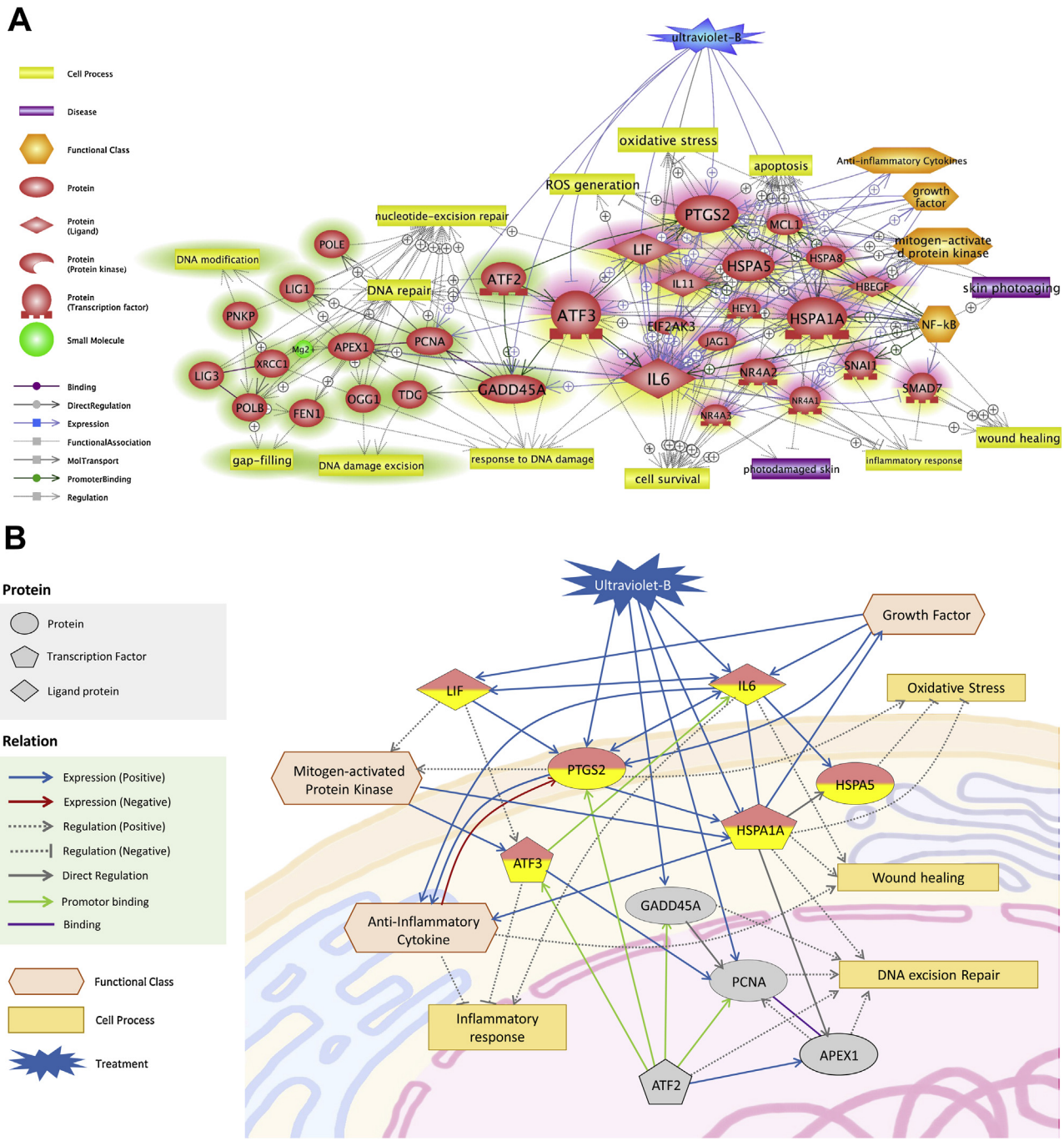

Fig. 2. Potential signaling networks associated with the photoprotective effects of visible red **light against UVB exposure. (A)** Results of the pathway analysis between common networks related to the biological benefits of visible red light (Fig. 1A) and data for another pathway related to the effectiveness of visible red light pretreatment against UVB (Fig. 1B). **(B)** We simplified meaningful paths in (A) pathway by considering the connectivity of each entity and confirmed reference literature of all paths in the pathway studio system. '+' or '−' at the end of the arrows in the pathway indicate positive/negative effects of each relations, respectively. Green highlights indicate genes involved in DNA excision repair pathways. Pink–yellow gradation indicates key genes involved in the protective effects of visible red light. A schematic legend of the entities and relations (marked as arrows) in the pathway are provided on the left side of the figure. Circles and squares on the arrows in the schematic legend are included to improve visibility.

selected for the analysis of protective pathways due to the scale of the transcriptomic changes (Supplementary Fig. 2).

We also observed that transcriptome changes induced by visible red light were partially preserved against UVB-induced influences during red light pretreatment. As summarized in Table 1, Red/Control pathway (Fig. 1A) and Pre-Red/UV pathway (Fig. 1B) have common cell processes and functional classes with meaningful common genes. We also observed that the common genes between both pathways had key roles with numerous connections in the protective pathway (Fig. 2A). Based on these findings, we infer that red light-induced interactions among the identified key genes (HSPA1A, HSPA5, PTGS2, IL-6, LIF, and ATF3) were maintained despite UVB-induced transcriptomic changes. This inference provided clues suggesting of a potential pathway underlying the photoprotective effect of red light (Fig. 2B), based on the careful curation of literature references using pathway analysis software. Our qRT-PCR validation results (Fig. 3) also support significance of our suggestion.

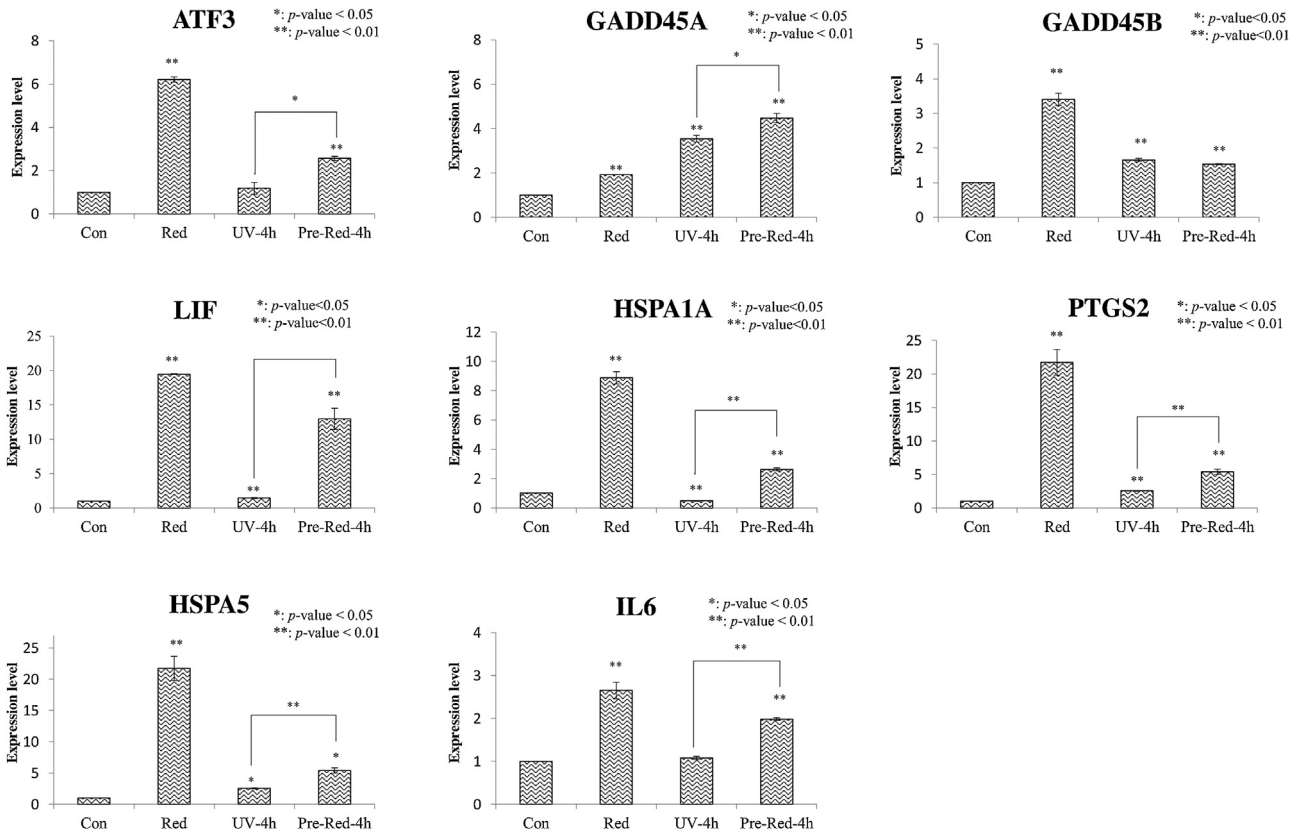

Fig. 3. mRNA level validation of selected genes related to the protective effects of visible red **light against UVB exposure.** Selected potential markers had similar changes in mRNA expression levels based on the RNA-seq results. The bars indicate means ± standard deviations; a single asterisk (*) and a double asterisks (**) represent *p*-values of less than 0.05 and 0.01, respectively.

UVB is causes severe oxidative stress, thereby damaging the DNA in skin cells, which can result in precancerous lesions [3,5,36]. Herein, we found close links between visible red light irradiation and DNA excision repair-related pathways (Figs. 1 and 2). GADD45A plays a crucial role in genomic stability by regulating cell cycle and apoptosis and stimulating DNA excision repair [37,38]. ATF3 is downstream of ATF2 and is reportedly a transcriptional regulator of GADD45A as well as a gatekeeper of genomic integrity upon UV-induced DNA damage [39]. GADD45B is a member of the GADD45 family of proteins, has a key role in DNA repair due to its ability to interact with PCNA, and is also involved in cell growth and apoptosis [40,41]. Major pathways in DNA excision repair processes are nucleotide excision repair (NER) and base excision repair (BER). NER is a representative mechanism to repair UV-induced bulk DNA lesions [42,43]. Additionally, studies have demonstrated the activity of BER against UV-induced oxidative damage [44]. Several *in vivo* and *in vitro* studies have reported red light-induced changes in BER-related mRNA expression in the skin [17,45]. Our previous study also demonstrated that visible red light irradiation of skin cells attenuates UV-induced cellular damage and enhances the GADD45A-mediated BER process [20]. In this context, our data indicate that visible red light enhances DNA repair processes, similar to previous studies using low-intensity infrared light [17,45]. The mRNA expression levels of ATF3 and GADD45A depend on visible red light treatment (Fig. 3); the activation of DNA repair signals induced by visible red light help to initiatie the repair processes in response to the UVB exposure of skin cells. This finding also supports our previous study, which demonstrated UVB-induced DNA damage attenuation by visible red light pre- and post-treatment in NHDFs and a three-dimensional skin model [20].

Taken together, our results suggest that the UVB-protective effects exerted by visible red light on human skin are involved in adaptive responses with enhanced maintenance of the redox and inflammatory signaling balance and activation of DNA excision repair processes. Additionally, we identified potential key networks and biomarker candidates that elucidate the photoprotective effect of visible red light. Our results corroborate with several *in vivo* and *in vitro* studies that investigated red light-induced repair and protective effects against skin damage. Moreover, our mechanistic suggestions regarding potential networks and key genes will be of considerable relevance for further research on the molecular mechanisms involved in visible red light photoprotection against UV-induced skin damage. These findings may facilitate the therapeutic application of visible red light in the dermatological cosmetic field.

Conflict of interests

The authors have no conflict of interest to declare.

Acknowledgement

This work was supported by the grant from the Amorepacific Corporation R&D Center, Yongin, Republic of Korea.

Appendix A. Supplementary data

Supplementary data associated with this article can be found, in the online version, at https://doi.org/10.1016/j.jdermsci.2019.03.003.

References

[1] R.P. Gallagher, T.K. Lee, Adverse effects of ultraviolet radiation: a brief review, Prog. Biophys. Mol. Biol. 92 (1) (2006) 119–131.
[2] A. Sarasin, The molecular pathways of ultraviolet-induced carcinogenesis, Mutat. Res. 428 (1–2) (1999) 5–10.
[3] M. Sato, C. Nishigori, M. Zghal, T. Yagi, H. Takebe, Ultraviolet-specific mutations in p53 gene in skin tumors in xeroderma pigmentosum patients, Cancer Res. 53 (13) (1993) 2944–2946.
[4] S. Kanjilal, W.E. Pierceall, K.K. Cummings, M.L. Kripke, H.N. Ananthaswamy, High frequency of p53 mutations in ultraviolet radiation-induced murine skin tumors: evidence for strand bias and tumor heterogeneity, Cancer Res. 53 (13) (1993) 2961–2964.
[5] E. Hodis, I.R. Watson, G.V. Kryukov, S.T. Arold, M. Imielinski, J.P. Theurillat, E. Nickerson, D. Auclair, L. Li, C. Place, D. Dicara, A.H. Ramos, M.S. Lawrence, K. Cibulskis, A. Sivachenko, D. Voet, G. Saksena, N. Stransky, R.C. Onofrio, W. Winckler, K. Ardlie, N. Wagle, J. Wargo, K. Chong, D.L. Morton, K. Stemke-Hale, G. Chen, M. Noble, M. Meyerson, J.E. Ladbury, M.A. Davies, J.E. Gershenwald, S. N. Wagner, D.S. Hoon, D. Schadendorf, E.S. Lander, S.B. Gabriel, G. Getz, L.A. Garraway, L. Chin, A landscape of driver mutations in melanoma, Cell 150 (2) (2012) 251–263.
[6] M. Widel, A. Krzywon, K. Gajda, M. Skonieczna, J. Rzeszowska-Wolny, Induction of bystander effects by UVA, UVB, and UVC radiation in human fibroblasts and the implication of reactive oxygen species, Free Radic. Biol. Med. 68 (2014) 278–287.
[7] S. Nishimura, Involvement of mammalian OGG1(MMH) in excision of the 8-hydroxyguanine residue in DNA, Free Radic. Biol. Med. 32 (9) (2002) 813–821.
[8] J. Hildesheim, D.V. Bulavin, M.R. Anver, W.G. Alvord, M.C. Hollander, L. Vardanian, A.J. Fornace Jr., Gadd45a protects against UV irradiation-induced skin tumors, and promotes apoptosis and stress signaling via MAPK and p53, Cancer Res. 62 (24) (2002) 7305–7315.
[9] W. Jiang, H.N. Ananthaswamy, H.K. Muller, M.L. Kripke, p53 protects against skin cancer induction by UV-B radiation, Oncogene 18 (29) (1999) 4247–4253.
[10] C.C. Franklin, S. Srikanth, A.S. Kraft, Conditional expression of mitogen-activated protein kinase phosphatase-1, MKP-1, is cytoprotective against UV-induced apoptosis, Proc. Natl. Acad. Sci. U. S. A. 95 (6) (1998) 3014–3019.
[11] A. Dube, C. Bock, E. Bauer, R. Kohli, P.K. Gupta, K.O. Greulich, He-Ne laser irradiation protects B-lymphoblasts from UVA-induced DNA damage, Radiat. Environ. Biophys. 40 (1) (2001) 77–82.
[12] R. Kohli, P.K. Gupta, Irradiance dependence of the He-Ne laser-induced protection against UVC radiation in E. coli strains, J. Photochem. Photobiol. B 69 (3) (2003) 161–167.
[13] P. Moore, T.D. Ridgway, R.G. Higbee, E.W. Howard, M.D. Lucroy, Effect of wavelength on low-intensity laser irradiation-stimulated cell proliferation in vitro, Lasers Surg. Med. 36 (1) (2005) 8–12.
[14] M.J. Conlan, J.W. Rapley, C.M. Cobb, Biostimulation of wound healing by low-energy laser irradiation. A review, J. Clin. Periodontol. 23 (5) (1996) 492–496.
[15] A. Gupta, T. Dai, M.R. Hamblin, Effect of red and near-infrared wavelengths on low-level laser (light) therapy-induced healing of partial-thickness dermal abrasion in mice, Lasers Med. Sci. 29 (1) (2014) 257–265.
[16] S.K. Kim, H.R. You, S.H. Kim, S.J. Yun, S.C. Lee, J.B. Lee, Skin photorejuvenation effects of light-emitting diodes (LEDs): a comparative study of yellow and red LEDs in vitro and in vivo, Clin. Exp. Dermatol. 41 (7) (2016) 798–805.
[17] Y. Zhang, S. Song, C.C. Fong, C.H. Tsang, Z. Yang, M. Yang, cDNA microarray analysis of gene expression profiles in human fibroblast cells irradiated with red light, J. Invest. Dermatol. 120 (5) (2003) 849–857.
[18] Z. Wang, M. Gerstein, M. Snyder, RNA-Seq: a revolutionary tool for transcriptomics, Nat. Rev. Genet. 10 (1) (2009) 57–63.
[19] B.J. Haas, A. Papanicolaou, M. Yassour, M. Grabherr, P.D. Blood, J. Bowden, M.B. Couger, D. Eccles, B. Li, M. Lieber, M.D. MacManes, M. Ott, J. Orvis, N. Pochet, F. Strozzi, N. Weeks, R. Westerman, T. William, C.N. Dewey, R. Henschel, R.D. LeDuc, N. Friedman, A. Regev, De novo transcript sequence reconstruction from RNA-seq using the Trinity platform for reference generation and analysis, Nat. Protoc. 8 (8) (2013) 1494–1512.
[20] Y.J. Kim, H.J. Kim, H.L. Kim, H.J. Kim, H.S. Kim, T.R. Lee, D.W. Shin, Y.R. Seo, A protective mechanism of visible red light in normal human dermal fibroblasts: enhancement of GADD45A-Mediated DNA repair activity, J. Invest. Dermatol. 137 (2) (2017) 466–474.
[21] C. Trapnell, L. Pachter, S.L. Salzberg, TopHat: discovering splice junctions with RNA-Seq, Bioinformatics 25 (9) (2009) 1105–1111.
[22] C. Trapnell, B.A. Williams, G. Pertea, A. Mortazavi, G. Kwan, M.J. van Baren, S.L. Salzberg, B.J. Wold, L. Pachter, Transcript assembly and quantification by RNA-Seq reveals unannotated transcripts and isoform switching during cell differentiation, Nat. Biotechnol. 28 (5) (2010) 511–515.
[23] A. Nikitin, S. Egorov, N. Daraselia, I. Mazo, Pathway studio–the analysis and navigation of molecular networks, Bioinformatics 19 (16) (2003) 2155–2157.
[24] K.J. Livak, T.D. Schmittgen, Analysis of relative gene expression data using real-time quantitative PCR and the 2(-Delta Delta C(T)) Method, Methods 25 (4) (2001) 402–408.
[25] K. Usui, T. Ikeda, Y. Horibe, M. Nakao, T. Hoshino, T. Mizushima, Identification of HSP70-inducing activity in Arnica montana extract and purification and characterization of HSP70-inducers, J. Dermatol. Sci. 78 (1) (2015) 67–75.
[26] C. Luo, E. Urgard, T. Vooder, A. Metspalu, The role of COX-2 and Nrf2/ARE in anti-inflammation and antioxidative stress: aging and anti-aging, Med. Hypotheses 77 (2) (2011) 174–178.
[27] T. Yoshida, N. Maulik, Y.S. Ho, J. Alam, D.K. Das, H(mox-1) constitutes an adaptive response to effect antioxidant cardioprotection: a study with transgenic mice heterozygous for targeted disruption of the Heme oxygenase-1 gene, Circulation 103 (12) (2001) 1695–1701.
[28] B.J. Erdle, S. Brouxhon, M. Kaplan, J. Vanbuskirk, A.P. Pentland, Effects of continuous-wave (670-nm) red light on wound healing, Dermatol. Surg. 34 (3) (2008) 320–325.
[29] T. Niu, Y. Tian, Q. Ren, L. Wei, X. Li, Q. Cai, Red light interferes in UVA-induced photoaging of human skin fibroblast cells, Photochem. Photobiol. 90 (6) (2014) 1349–1358.
[30] C. Marionnet, C. Tricaud, F. Bernerd, Exposure to non-extreme solar UV daylight: spectral characterization, effects on skin and photoprotection, Int. J. Mol. Sci. 16 (1) (2014) 68–90.
[31] T. Hai, C.C. Wolford, Y.S. Chang, ATF3, a hub of the cellular adaptive-response network, in the pathogenesis of diseases: is modulation of inflammation a unifying component? Gene Expr. 15 (1) (2010) 1–11.
[32] S.A. Ali, G. Kaur, J.K. Kaushik, D. Malakar, A.K. Mohanty, S. Kumar, Examination of pathways involved in leukemia inhibitory factor (LIF)-induced cell growth arrest using label-free proteomics approach, J. Proteomics 168 (2017) 37–52.
[33] K.J. O'Byrne, A.G. Dalgleish, Chronic immune activation and inflammation as the cause of malignancy, Br. J. Cancer 85 (4) (2001) 473–483.
[34] A. Cekici, A. Kantarci, H. Hasturk, T.E. Van Dyke, Inflammatory and immune pathways in the pathogenesis of periodontal disease, Periodontol. 2000 64 (1) (2014) 57–80.
[35] T. Lawrence, D.A. Willoughby, D.W. Gilroy, Anti-inflammatory lipid mediators and insights into the resolution of inflammation, Nat. Rev. Immunol. 2 (10) (2002) 787–795.
[36] E. Pelle, X. Huang, T. Mammone, K. Marenus, D. Maes, K. Frenkel, Ultraviolet-B-induced oxidative DNA base damage in primary normal human epidermal keratinocytes and inhibition by a hydroxyl radical scavenger, J. Invest. Dermatol. 121 (1) (2003) 177–183.
[37] T. Maeda, A.N. Hanna, A.B. Sim, P.P. Chua, M.T. Chong, V.A. Tron, GADD45 regulates G2/M arrest, DNA repair, and cell death in keratinocytes following ultraviolet exposure, J. Invest. Dermatol. 119 (1) (2002) 22–26.
[38] M.L. Smith, I.T. Chen, Q. Zhan, I. Bae, C.Y. Chen, T.M. Gilmer, M.B. Kastan, P.M. O'Connor, A.J. Fornace Jr., Interaction of the p53-regulated protein Gadd45 with proliferating cell nuclear antigen, Science 266 (5189) (1994) 1376–1380.
[39] L. Turchi, M. Fareh, E. Aberdam, S. Kitajima, F. Simpson, C. Wicking, D. Aberdam, T. Virolle, ATF3 and p15PAF are novel gatekeepers of genomic integrity upon UV stress, Cell Death Differ. 16 (5) (2009) 728–737.
[40] J.S. Park, S.J. Park, X. Peng, M. Wang, M.A. Yu, S.H. Lee, Involvement of DNA-dependent protein kinase in UV-induced replication arrest, J. Biol. Chem. 274 (45) (1999) 32520–32527.
[41] O. Kovalsky, F.D. Lung, P.P. Roller, A.J. Fornace Jr., Oligomerization of human Gadd45a protein, J. Biol. Chem. 276 (42) (2001) 39330–39339.
[42] T. Nouspikel, DNA repair in mammalian cells : Nucleotide excision repair: variations on versatility, Cell. Mol. Life Sci. 66 (6) (2009) 994–1009.
[43] J. D'Orazio, S. Jarrett, A. Amaro-Ortiz, T. Scott, UV radiation and the skin, Int. J. Mol. Sci. 14 (6) (2013) 12222–12248.
[44] S.N. Kassam, A.J. Rainbow, UV-inducible base excision repair of oxidative damaged DNA in human cells, Mutagenesis 24 (1) (2009) 75–83.
[45] A. de Souza da Fonseca, A.L. Mencalha, V.M. Araujo de Campos, S.C. Ferreira Machado, A.A. de Freitas Peregrino, M. Geller, F. de Paoli, DNA repair gene expression in biological tissues exposed to low-intensity infrared laser, Lasers Med. Sci. 28 (4) (2013) 1077–1084.